Atmos. Meas. Tech. Discuss., 3, 2633–2649, 2010
www.atmos-meas-tech-discuss.net/3/2633/2010/
doi:10.5194/amtd-3-2633-2010
© Author(s) 2010. CC Attribution 3.0 License.

Atmospheric Measurement Techniques Discussions

This discussion paper is/has been under review for the journal Atmospheric Measurement Techniques (AMT). Please refer to the corresponding final paper in AMT if available.

Retrieval of atmospheric optical parameters from ground-based sun-photometer measurements for Zanjan, Iran

A. Bayat, A. Masoumi, and H. R. Khalesifard

Institute for Advanced Studies in Basic Sciences (IASBS), Iran

Received: 29 April 2010 – Accepted: 1 June 2010 – Published: 17 June 2010

Correspondence to: A. Bayat (a_bayat@iasbs.ac.ir)

Published by Copernicus Publications on behalf of the European Geosciences Union.

Abstract

We are reporting the results of ground-based spectroradiometric measurements on aerosols and water vapor in the atmosphere of Zanjan for the period of October 2006 to September 2008 using a Cimel CE318-2 sun-photometer. Zanjan is a city in Northwest Iran, located at 36.70° N, 48.51° E, and at an altitude of 1800 above m.s.l. The spectral aerosol optical depth, Ångström exponent, and columnar water vapor have been calculated using the data recorded by the sunphotometer through direct-beam irradiance measurements of sunlight (sun mode). The average values of aerosol optical depth at 440 nm, columnar water vapor, and the Ångström exponent, α, during the mentioned period are measured as, 0.27±0.16, 0.53±0.37 cm and 0.75±0.46, respectively. The maximum (minimum) value of the aerosol optical depth was recorded in May 2007 (January 2007), and that of columnar water vapor, in July 2007 (January 2008). Using the least-squares method, the Ångström exponent was calculated in the spectral interval 440–870 nm along with the coefficients of a second order polynomial fit (α_1 and α_2) to the log-log plot of aerosol optical depth versus the wavelength. The coefficient α_2 shows that most of the aerosols in the Zanjan area have dimensions larger than 1 µm. The values calculated for $\alpha_2 - \alpha_1$ indicate that 70% of the aerosols are in the coarse-mode (>1 µm) and 30% of them are in the fine-mode (<1 µm). Comparison of $\alpha_2 - \alpha_1$ for the atmosphere over Zanjan with other regions indicates dust and anthropogenic aerosols are the most dominant aerosols in the region.

1 Introduction

Iran, a country in the Middle East, is located within the Earth's dust belt. The Tigris and Euphrate basins in the west, and the Arabian Peninsula in the south are the main dust sources, as frequently observed in these regions (Prospero et al., 2002). Even though other observations show that other sources within the country, such as the Qom lake (a salt-covered playa) in the center (Mortazavi, 2009), or Hamoun Jaz-Murian in the

AMTD
3, 2633–2649, 2010

south east have some impact on the atmospheric aerosols in Iran (Leon and Legrand, 2003), outside sources are more dominant.

Zanjan is a city in Northwest Iran (36.70° N, 48.51° E, 1800 above m.s.l.), located in a mountainous region. It is subject to frequent dust storms especially in mid and late spring as well as late summer and early fall. A free horizon terrace and excellent weather conditions, with 2850 h of sun per year (Samimi et al., 1997), make this area adequate for aerosol monitoring with remote sensing instruments. The aerosol optical depth (AOD), which is the integral of the optical extinction coefficient of the atmospheric aerosols from the surface to the top of the atmosphere, is an important parameter for visibility degradation (due to atmospheric pollution), solar radiation extinction, climate effects, and tropospheric corrections in remote sensing (Dubovik et al., 2002). Here we are reporting the measurements on the aerosol optical depth of the atmosphere of Zanjan using an automatic sun-tracker sun-photometer CIMEL CE318-2. The measurements were carried out in the period between October 2006 and the end of September 2008.

Recorded data on the 936 nm wavelength channel of the sunphotometer (SPM) in combination with the measurements on the 870 nm and 1020 nm wavelength channels provide a measure of the columnar water vapor (CWV) (Halthore et al., 1997). The Ångström exponent, α, is often used as a qualitative indicator of aerosol particle size (Ångström, 1929). Using the least-squares method, α was calculated in the spectral interval 440–870 nm. We also used a second order polynomial fit to the log-log plot of AOD versus wavelength (Kaskaoutis et al., 2007) to have a more accurate measure of aerosol size distribution in the atmosphere of Zanjan.

In the next parts of this manuscript, after introducing the measurement instrument in Sect. 2, the theoretical basis of the work and calculations will be presented in Sect. 3. Section 4 contains the results of the measurements, and finally the work is concluded in Sect. 5.

AMTD
3, 2633–2649, 2010

2 Measurements and instrumentation

The SPM records the sun and sky irradiance on the photometer surface at eight wavelength channels, 440, 670, 870, 936, and 1020 nm where the 870 nm channels consist of one non-polarized and three polarized channels to provide the Stokes parameters. These channels are selected wavelengths that have minimal molecular absorption except for the 936 nm channel that matches one of the water vapor absorption lines (Holben et al., 1998).

The SPM is installed at the Institute for Advanced Studies in Basic Sciences, IASBS, (36.70° N, 48.51° E, 1800 m above m.s.l.) and from now on we call it the IASBS site.

3 Methods

3.1 Aerosol optical depth

Atmospheric transmittance is a function of the attenuation of extra-terrestrial irradiance by scattering and absorption. When the direct beam is measured over a narrow band-pass (strictly, monochromatic radiation) the Beer-Lambert-Bouguer attenuation law holds and the instantaneous, total optical depth for that wavelength, τ_λ, can be derived from:

$$I_\lambda = \frac{I_{0\lambda}}{R^2} \exp(-m\tau_\lambda). \quad (1)$$

Where, I_λ is the intensity of the solar irradiance over the SPM, $I_{0\lambda}$ is a measure of solar radiation behind the atmosphere that can be found by drawing a Langly plot for the instrument (Holben et al., 1998). R is the Earth-Sun distance in Astronomical Units at the time of observation and m is the relative optical air mass, which is approximated as the secant of the solar-zenith angle (Kasten et al., 1989). The total optical depth, τ_λ, is the result of attenuation by molecules (Rayleigh scattering), aerosols (Mie scattering), and absorption by atmospheric gasses like water vapor and other uniformly mixed

AMTD
3, 2633–2649, 2010

gases. Each of these components can be separated. The Rayleigh optical depth, $\tau_{\text{Rayleigh},\lambda}$, as a part of τ_λ is readily calculated, depending only on the wavelength and barometric pressure at the surface (Holben et al., 1998). The aerosol optical depth, $\tau_{\text{Aerosol},\lambda}$, can be obtained through:

$$\tau_{\text{Aerosol},\lambda} = \tau_\lambda - \tau_{\text{Rayleigh},\lambda}. \quad (2)$$

3.2 Water vapor

Extraction of atmospheric columnar water vapor amount from the SPM measurements generally relies on measurements in 936 nm channel of the SPM that coincides with one of the water vapor absorption bands. The aerosol effect is removed by interpolation between the two adjacent bands of the SPM (870 and 1020 nm wavelength channels) (Halthore et al., 1997) and subtracting the calculated $\tau_{\text{Aerosol},\lambda=936\text{nm}}$ from the measured $\tau_{\lambda=936\text{nm}}$. In this case, Eq. (1) is not valid anymore since the exponential attenuation applies strictly to monochromatic radiation and is invalid across the broad region of the water vapor absorption band.

Atmospheric radiation transmission in the water vapor band T_w can be modelled as (Halthore et al., 1997),

$$T_w = \exp(-am^b w^b), \quad (3)$$

where w is the water vapor vertical column abundance measured in cm and a and b are constants that depend on the wavelength, transmittance spectrum of the SPM filter, and atmospheric conditions (temperature-pressure lapse and the vertical profile of water vapor band).

Halthore (1997) showed that for a narrow band (less than 10 nm) filter, sensitivity to the atmosphere can be removed. A modified-Langley method is used for deriving calibration values for the water vapor absorption band around 936 nm (Bruegge et al., 1992).

AMTD
3, 2633–2649, 2010

3.3 Ångström exponent

Ångström (1929) proposed an empirical formula to approximate the spectral dependence of atmospheric extinction caused by aerosols:

$$\tau_{\text{Aerosol},\lambda} = \beta\lambda^{-\alpha}, \quad (4)$$

where β is the Ångström's turbidity coefficient which is equal to the AOD at λ=1 µm, and α is the widely known Ångström exponent. Although in this definition α and β are wavelength independent, it is well known that both parameters depend on the wavelength.

A more precise empirical relationship between aerosol extinction coefficient and wavelength is obtained by using a second-order polynomial (King et al., 1976),

$$\ln\tau_{\text{Aerosol},\lambda} = \alpha_0 + \alpha_1 \ln\lambda + \alpha_2 \ln\lambda^2, \quad (5)$$

where the coefficient α_2 accounts for a curvature often observed in sun-photometry measurements when $\tau_{\text{Aerosol},\lambda}$ is plotted against the wavelength on a log-log scale. The curvature can be an indicator of the aerosol particle size. A negative (positive) curvature indicates aerosol size distribution dominated by fine (coarse) mode particles (Eck et al., 2001a,b; Schuster et al., 2006).

In retrieving the data recorded by a SPM, the second-order polynomial fit (Eq. 5) is usually applied to the AOD values at three wavelengths 440, 675, and 870 nm. The AOD's at 1020 nm are not included because of possible water vapor absorption effects at that wavelength, resulting in inaccuracies in the computation of the second order polynomial fit and estimation of the values of α_1 and α_2 parameters (Eck et al., 2001a).

Schuster et al. (2006) reported that for $\alpha_2-\alpha_1<1$ aerosol size distributions are dominated by the coarse mode (>1 µm) aerosols. The occurrence of $\alpha_2-\alpha_1>2$ represents an aerosol size distributions dominated by fine mode (<1 µm) particles and when $1<\alpha_2-\alpha_1<2$ most of the aerosols are in the fine mode.

AMTD
3, 2633–2649, 2010

4 Results

In this work, only the SPM data in the sun-mode have been used. In the sun-mode, the SPM looks directly at the sun at a viewing solid angle of 1.2° and measures the atmospheric optical depth.

4.1 Aerosol optical depth climatology

Figure 1 shows the AOD (440 nm) variations for two years of available cloud-free data. A main feature of the AOD is its high variability. The variability is higher for lower wavelengths. The occurrence of high turbidity events is higher during spring, as can be seen for example in 2007, where consecutive peaks resulted from the considerable number of desert dust events between April and June (Fig. 1).

Once the main features of the individual measurements were observed, daily and monthly averages were calculated in order to get climatological values for the AOD. Figure 2 shows the AOD monthly averages for 440 nm channel during the two years. The variability is indicated by the standard deviation within the month (error bars).

The pattern of low AOD during winter times is clear in Fig. 2, when the minimum value of $\tau_{\mathrm{Aerosol},\lambda}$=0.15, occurred in January 2007. These low levels of aerosol loading are due to more frequent rains in winter and few occurrences of desert events. On the other hand, during spring and summer the AOD values are above 0.25 and even get close to 0.40 during April and May 2007 and April 2008, with much higher variability indicated by larger error bars.

The turbidity of the atmosphere increases because of the characteristic spring and summer dry seasons in Zanjan and also by most frequent desert dust outbreaks over this area. These events mostly happen every spring and summer, although their number and intensity shows a high variation from year to year. We can observe two AOD maxima during the year: the first one in spring, and the second at the end of the summer (Fig. 2). It can also be noticed that the AOD remains low from October to January with a decreasing pattern after the summer and an increasing one after the winter while

AMTD
3, 2633–2649, 2010

it has almost the same behavior throughout the two years.

The described behavior is more or less the same for all wavelength channels of the SPM (not shown). The general statistics for the whole data series are summarized in Table 1. For the whole data set the average AOD (440 nm) is 0.27 and the standard deviation is 0.16, representing a 50% variation. At 1020 nm the average AOD decreases to 0.15, showing a moderate wavelength dependence of the AOD (Table 1).

4.2 Columnar water vapor climatology

The temporal resolution of the recorded data set allows one to study the temporal evolution of the CWV. Figure 3 shows the CWV (936 nm) variation along the two years for cloud-free available data. The results show that the maximum (minimum) CWV occurred in July and August (December, January, and February). The high levels of CWV loading are due to sunshine in the summer. The average CWV is 0.53 cm for the whole period of the data recording.

4.3 Aerosol classification, Ångström exponent

Since the spectral shape of the extinction is related to the particle size, the Ångström exponent is commonly used as an indicator of the predominant aerosol size (type) (Ångström, 1929). A more precise relation between the aerosol extinction and wavelength is a second order polynomial fit (Eq. 5) (King et al., 1976). Variations of α_2 and $\alpha_2 - \alpha_1$ versus AOD are more precise tools for aerosol classification (Kaskaoutis et al., 2007). While the AOD gives information about the aerosol loading, and α_2 and $\alpha_2 - \alpha_1$ are related to the aerosol size (type), joint analysis of these parameters makes an interpretation of the data possible (Kaskaoutis et al., 2007). The correlation between α_2 and AOD (440 nm) provides information on the atmospheric conditions under which the spectral variation of α_2 is negligible and so the spectral variation of AOD can be accurately described by the simple Ångström formula.

Figure 4 shows the correlation between the coefficient α_2 computed in the spectral

AMTD
3, 2633–2649, 2010

interval 440–870 nm and the measured AOD (440 nm) for the IASBS site from October 2006 to September 2008. There is a decreasing trend in α_2 with increasing AOD (440 nm). Ångström exponent and α_2 coefficients show that most aerosols in the atmosphere of Zanjan are in the coarse mode. In Fig. 5, $\alpha_2-\alpha_1$ values are plotted against AOD (440 nm) for the IASBS site during the mentioned period.

Kaskaoutis et al. (2007) reported the variations of $\alpha_2-\alpha_1$ versus the AOD for four different AERONET sites, Alta Floresta (Brezil) a rural site directly influenced by biomass burning smoke during the fire season, Ispera (Italy) an urban/industrial area with significant anthropogenic and industrial activities, Nauru a remote island in the tropical Pacific characterized by very small aerosol loading, and Solar Village (Saudi Arabia) a continental remote site with significant contribution of desert dust particles. Our results in Fig. 5 show a considerable similarity with the superposition of reported data from Solar Village and Ispera.

It should be noted that because of the geographical location of Zanjan, the maritime and biomass burning aerosols will not have a considerable impact on its atmosphere. So, one may conclude that dust and anthropogenic aerosols are the main sources of the aerosol in the atmosphere of Zanjan. The calculated values of $\alpha_2-\alpha_1$ show that 70% of the aerosols in Zanjan's atmosphere are in the coarse mode and 30% in the fine mode.

It can be seen from Fig. 5 for clean conditions, i.e. small AOD (440 nm) that there is a wide range of $\alpha_2-\alpha_1$ values (from −0.13 to 3.07) for all aerosol types. This is an indication of the existence of bimodal-size distributions at relatively low optical depths.

5 Conclusions

The IASBS site has the only SPM operating in a region covered by Iran and Iraq. The 2-year data series presented here allows for the first time a climatological approach in the study of AOD, CWV, and Ångström exponent. The average AOD (440 nm) and CWV for the mentioned period were 0.27, 0.53 cm, respectively. The maximum (minimum)

AMTD
3, 2633–2649, 2010

aerosol optical depth was recorded in May 2007 (January 2007), and the maximum (minimum) CWV occurred in summer (winter). A classification for the different aerosol types appearing in Zanjan's atmosphere has been proposed based on the analysis of the AOD and Ångström exponent features.

A comparison of $\alpha_2 - \alpha_1$ for Zanjan's atmosphere and the SPM measurements for other regions indicates that the dust and anthropogenic aerosols are the most dominant aerosols in the region.

References

Ångström, A. K.: On the atmospheric transmission of sun radiation and on the dust in the air, Geogr. Ann., 12, 130–159, 1929. 2635, 2638, 2640

Bruegge, C. T., Conel, J. E., Green, R. O., Margolis, J. S., Holm, R. G., and Toon, G.: Water vapor column abundance retrievals during FIFE, J. Geophys. Res., 97, 18759–18768, 1992. 2637

Dubovik, O., Holben, B. N., Eck, T. F., Smirnov, A., Kaufman, Y. J., King, M. D., Tanré, D., and Slutsker, I.: Variability of absorption and optical properties of key aerosol types observed in worldwide locations, J. Atmos. Sci., 59, 590–608, 2002. 2635

Eck, T. F., Holben, B. N., Dubovic, O., Smirnov, A., Slutsker, I., Lobert, J. M., and Ramanathan, V.: Column-integrated aerosol optical properties over the Maldives during the northeast monsoon for 1998–2000, J. Geophys. Res., 106, 28555–28566, 2001a. 2638

Eck, T. F., Holben, B. N., Ward, D. E., Dubovic, O., Reid, J. S., Smirnov, A., Mukelabai, M. M., Hsu, N. C., O'Neil, N. T., and Slutsker, I.: Characterization of the optical properties of biomass burning aerosols in Zambia during the 1997 ZIBBEE field campaign, J. Geophys. Res., 106(D4), 3425–3448, 2001b. 2638

Holben, B. N., Eck, T. F., Slutsker, I., Tanre, D., Buis, J. P., Setzer, A., Vermote, E., Reagan, J. A., Kaufman, Y. J., Nakajima, T., Lavenu, F., Jankowiak, I., and Smirnov, A.: AERONET – a federated instrument network and data archive for aerosol characterization, Remote Sens. Environ., 66, 1–16, 1998. 2636, 2637

Halthore, R, N., Eck, T. F., Holben, B. N., and Markham, B. L.: Sun-photometric measurements

AMTD
3, 2633–2649, 2010

of atmospheric water vapour column abundance in the 940-nm band, J. Geophys. Res., 102, 4343–4352, 1997. 2635, 2637
Kaskaoutis, D. G., Kambezidis, H. D., Hatzianastassiou, N., Kosmopoulos, P. G., and Badarinath, K. V. S.: Aerosol climatology: dependence of the Angstrom exponent on wavelength over four AERONET sites, Atmos. Chem. Phys. Discuss., 7, 7347–7397, doi:10.5194/acpd-7-7347-2007, 2007. 2635, 2640, 2641
Kasten, F. and Young, A. T.: Revised optical air mass tables and approximation formula, Appl. Optics, 28, 4735–4738, 1989. 2636
King, M. D. and Byrne, D. M.: A method for inferring total ozone content from spectral variation of total optical depth obtained with a solar radiometer, J. Atmos. Sci., 33, 2242–2251, 1976. 2638, 2640
Leon, J. and Legrand, M.: Mineral dust sources in the surrounding of the North Indian Ocean, Geophys. Res. Lett., 30(6), 1309, 2003. 2635
Mortazavy, F.: Characterizing the resources and type of aerosols in the Zanjan atmosphere using the data recorded by a sun-photometer, Hysplit4 and Giovanni Models, M.Sc., IASBS, Zanjan, Iran, 2009. 2634
Prospero, J. M., Ginoux, P., Torres, O., Nicholson, S. E., and Gill, T. E.: Environmental characterization of global sources of atmospheric soil dust identified with the NIMBUS 7 Total Ozone Mapping Spectrometer (TOMS) absorbing aerosol product, Rev. Geophys., 40, 1002–1029, 2002. 2634
Samimi, J. and Anvari, A.: Envestigation and analysis of solar energy information and its potantioal in Iran, Tech. Report, Center for Energy Studies, Iran, 1997. 2635
Schuster, G. L., Dubovik, O., and Holben, B. N.: Ångström exponent and bimodal aerosol size distributions, J. Geophys. Res., 111, 07207, 14 pp., 2006. 2638

AMTD
3, 2633–2649, 2010

Table 1. Statistics for the 2-year data series in Zanjan, AOD in all 4 wavelength channels of the SPM, CWV at 936 nm, α, α_2 and $\alpha_2-\alpha_1$; the average, standard deviation (STD), minimum, and maximum; total. Total number of days with data: 431.

	AOD_{440}	AOD_{670}	AOD_{870}	AOD_{1020}	CWV (cm)	α	α_2	$\alpha_2-\alpha_1$
Average	0.27	0.19	0.19	0.15	0.53	0.75	1.43	0.77
STD	0.16	0.14	0.14	0.14	0.37	0.46	1.13	0.47
Min	0.03	0.01	0.01	0.01	0.01	−0.13	−2.29	−0.13
Max	0.87	0.68	0.66	0.68	1.63	2.94	8.47	3.07

AMTD
3, 2633–2649, 2010

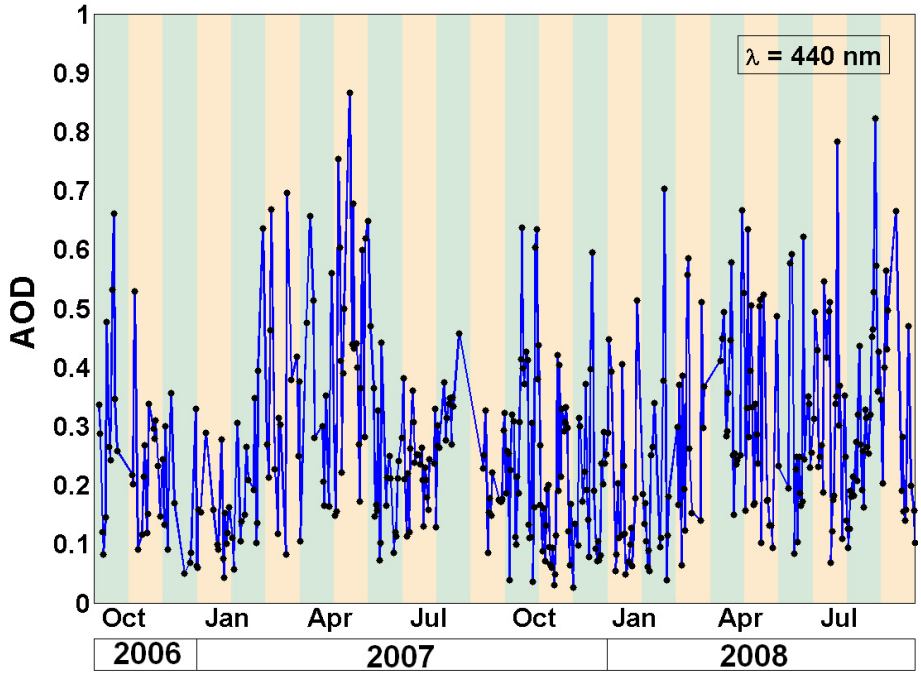

Fig. 1. Temporal evolution of AOD (440 nm) daily averages in Zanjan, October 2006 to September 2008, IASBS site.

AMTD
3, 2633–2649, 2010

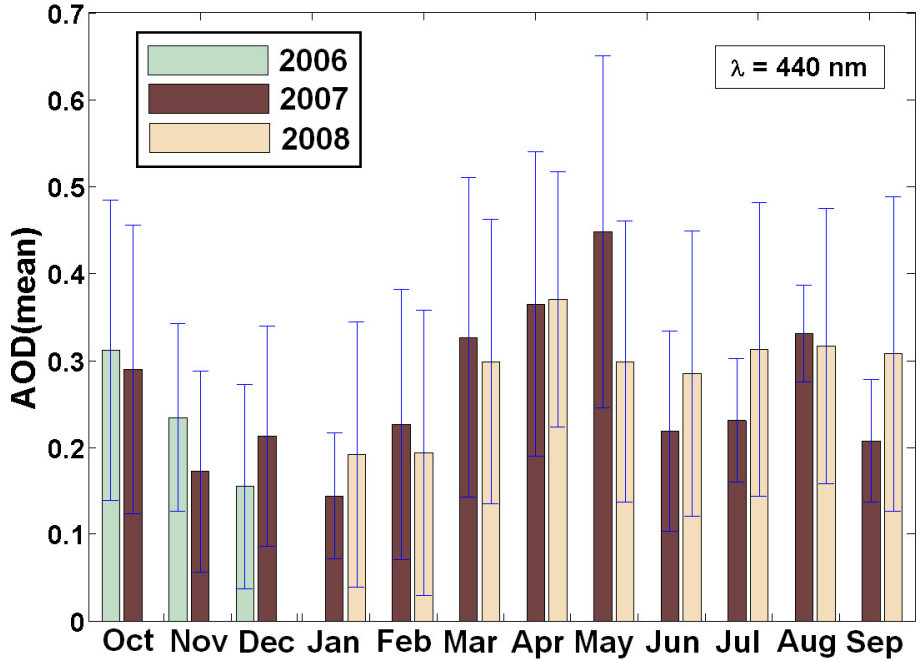

Fig. 2. Temporal evolution of AOD (440 nm), monthly averages in Zanjan for the period of October 2006 to September 2008, IASBS site.

AMTD
3, 2633–2649, 2010

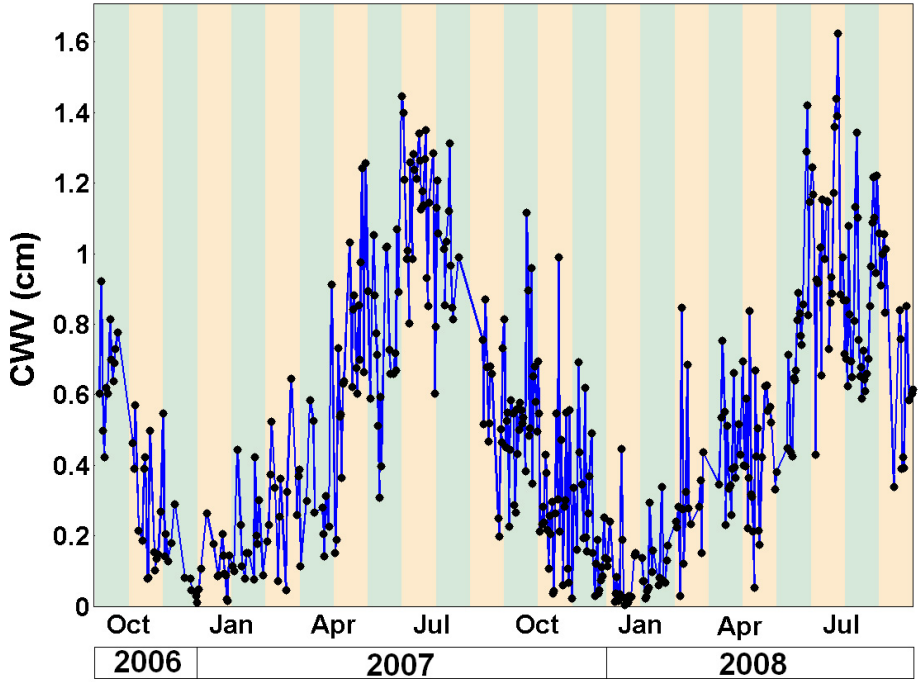

Fig. 3. Temporal evolution of CWV (936 nm) daily averages in Zanjan, October 2006 to September 2008, IASBS site.

AMTD
3, 2633–2649, 2010

Atmospheric optical parameters measurements for Zanjan, Iran

A. Bayat et al.

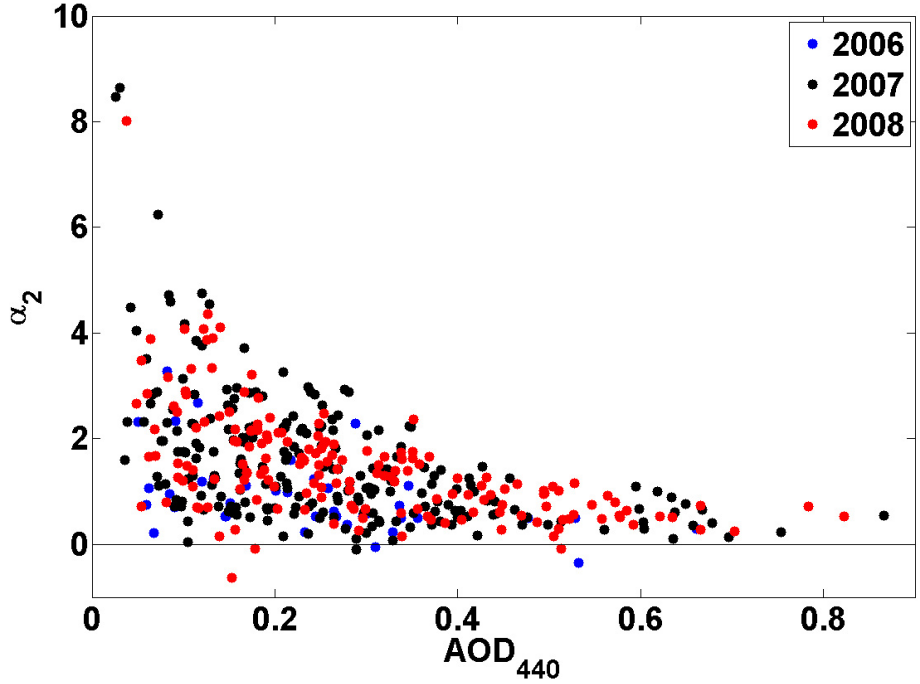

Fig. 4. Correlation between the coefficient α_2 computed in the spectral interval 440–870 nm and AOD (440 nm), IASBS site, October 2006 to September 2008.

AMTD
3, 2633–2649, 2010

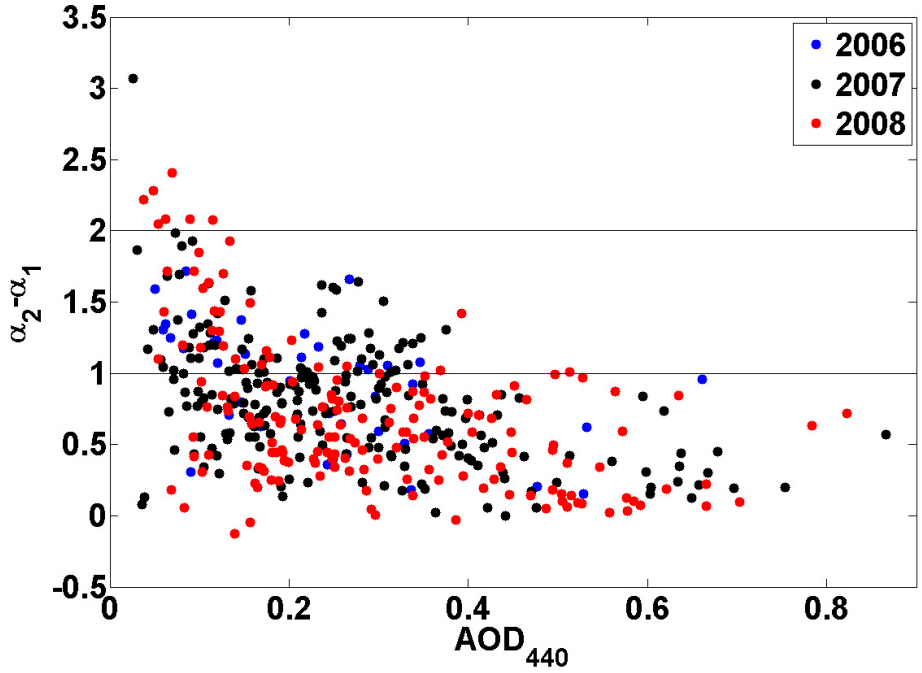

Fig. 5. Correlation between the coefficient $\alpha_2 - \alpha_1$ computed in the spectral interval 440–870 nm and AOD (440 nm), IASBS site, October 2006 to September 2008.

AMTD
3, 2633–2649, 2010